PROCEEDINGS OF SPIE

SPIEDigitalLibrary.org/conference-proceedings-of-spie

Optical modeling for the LiteBIRD Medium and High Frequency Telescope

L. Lamagna, C. Franceschet, M. De Petris, J. Gudmundsson, P. Hargrave, et al.

L. Lamagna, C. Franceschet, M. De Petris, J. E. Gudmundsson, P. Hargrave, B. Maffei, F. Noviello, C. O'Sullivan, A. Paiella, F. Columbro, J. Austermann, M. Bersanelli, A. Chahadih, M. Cicuttin, L. Clermont, P. de Bernardis, K. Fleury-Frenette, M. P. Georges, C. Geuzaine, J. Hastanin, S. Henrot-Versillé, J. Hubmayr, G. Jaehnig, R. Keskitalo, S. Masi, F. Matsuda, T. Matsumura, L. Montier, B. Mot, F. Piacentini, G. Pisano, J. Y. Plesseria, A. Ritacco, G. Savini, A. Shitvov, A. Suzuki, N. Trappe, B. Winter, "Optical modeling for the LiteBIRD Medium and High Frequency Telescope," Proc. SPIE 12190, Millimeter, Submillimeter, and Far-Infrared Detectors and Instrumentation for Astronomy XI, 121901R (31 August 2022); doi: 10.1117/12.2629271

SPIE.

Event: SPIE Astronomical Telescopes + Instrumentation, 2022, Montréal, Québec, Canada

Optical modeling for the LiteBIRD Medium & High Frequency Telescope

L. Lamagna[a,b], C. Franceschet[c,d], M. De Petris[a,b], J.E. Gudmundsson[e], P. Hargrave[f], B. Maffei[g], F. Noviello[f], C. O'Sullivan[h], A. Paiella[a,b], F. Columbro[a,b], J. Austermann[i], M. Bersanelli[c,d], A. Chahadih[g], M. Cicuttin[j], L. Clermont[j], P. de Bernardis[a,b], K. Fleury[j], M.P. Georges[j], C. Geuzaine[j], J. Hastanin[j], S. Henrot-Versillé[k], J. Hubmayr[i], G. Jaehnig[l], R. Keskitalo[m], S. Masi[a,b], F. Matsuda[n], T. Matsumura[o], L. Montier[p], B. Mot[p], F. Piacentini[a,b], G. Pisano[a], J.Y. Plesseria[j], A. Ritacco[q], G. Savini[r], A. Shitvov[r], A. Suzuki[s], N. Trappe[h], and B. Winter[t]

[a]Physics Department, Sapienza University of Rome, Italy
[b]INFN Sezione di Roma1, Italy
[c]Physics Department, Università degli Studi di Milano Statale, Italy
[d]INFN Sezione di Milano, Italy
[e]The Oskar Klein Centre, Department of Physics, Stockholm University, Sweden
[f]School of Physics and Astronomy, Cardiff University, UK
[g]Université Paris-Saclay, CNRS, Institut d'Astrophysique Spatiale, 91405, Orsay, France
[h]Department of Experimental Physics, Maynooth University, Ireland
[i]National Institute of Standards and Technology, Boulder, Colorado, US
[j]Centre Spatial de Liège, Université de Liège, Belgium
[k]Université Paris-Saclay, CNRS/IN2P3, IJCLab, Orsay, France
[l]Center for Astrophysics and Space Astronomy, University of Colorado Boulder, US
[m]Computational Cosmology Center, Lawrence Berkeley National Lab, US
[n]ISAS JAXA, Sagamihara, Kanagawa 252-5210, Japan
[o]Kavli Institute for the Physics and Mathematics of the Universe, Kashiwa, Japan
[p]Institut de Recherche en Astrophysique et Planétologie, Toulouse, France
[q]INAF, Osservatorio Astronomico di Cagliari, Cagliari, Italy
[r]Department of Physics and Astronomy, University College London, UK
[s]Physics Division, Lawrence Berkeley National Lab, US
[t]Department of Space and Climate Physics, University College London, UK

ABSTRACT

LiteBIRD is the next-generation space mission for polarization-sensitive mapping of the Cosmic Microwave Background anisotropies, with observations covering the full sky in a wide frequency range (34-448 GHz) to ensure high-precision removal of polarized foregrounds. Its main goal is to constrain the contribution of primordial gravitational waves to the curly component of the CMB polarization pattern. The LiteBIRD Medium and High Frequency Telescope (MHFT) will observe the sky in the 89-448 GHz band. Its optical configuration features two separate dual-lens assemblies with 300mm and 200mm apertures, 28° fields of view and diffraction-limited imaging over the whole spectral range. Polarization modulation is achieved through the continuous spinning of a half-wave plate at the optical entrance of each system. The optical studies for MHFT focus on a refined modeling of the telescope elements (lenses, anti-reflection coatings, absorbers, interfaces) to assess their individual effects on the predicted optical behavior of the telescopes. Such studies will provide key inputs for end-to-end simulations

Corresponding authors e-mail:
luca.lamagna@uniroma1.it, cristian.franceschet@fisica.unimi.it

Millimeter, Submillimeter, and Far-Infrared Detectors and Instrumentation for Astronomy XI, edited by Jonas Zmuidzinas, Jian-Rong Gao, Proc. of SPIE Vol. 12190, 121901R · © 2022 SPIE · 0277-786X · doi: 10.1117/12.2629271

and will inform the subsystem and system-level characterization to meet the stringent requirements set for the LiteBIRD success. We describe the progress in MHFT optical modeling and the ongoing efforts to reproduce full Medium Frequency Telescope (MFT) and High Frequency Telescope (HFT) beams for representative focal plane pixels down to the far-sidelobe angular region. Here, systematic effects due to challenging beam measurements and higher order optical coupling between the telescope and the surrounding structures are likely to affect the final level and shape of the beams and thus set compelling requirements for in-flight calibration and beam reconstruction.

Keywords: LiteBIRD, Cosmic Microwave Background, polarization measurements, millimeter wavelengths, refractive telescopes, space telescopes, optical modeling

1. INTRODUCTION

The measurement of the polarization of the Cosmic Microwave Background (CMB) radiation is one of the current frontiers in observational cosmology. In particular, the detection of the primordial divergence-free component of the polarization field, the B-mode, could reveal the presence of gravitational waves in the early Universe. The detection of such a component is at the moment the most promising technique to probe the inflationary theory describing the very early evolution of the Universe.

B-mode polarization in the CMB is produced by tensor perturbations generated during cosmic inflation in the very early Universe.[1,2] The level of this signal is unknown: current inflation models are unable to provide a firm reference value. However, the detection of this signal would be of utmost importance, providing a way to measure the energy-scale of inflation and a window on a physical regime characterized by extremely high energies. Knowledge of the energy scale of inflation also has important implications for several other aspects of fundamental physics, such as axions and, in the context of string theory, the fields that control the shapes and sizes of the compact dimensions.

The search for primordial B-modes is made even more complex by the level of its contribution to the linear polarization anisotropy in the CMB: the *rms* level of CMB temperature anisotropy is of the order of 100 µK, the *rms* level of the gradient component of CMB polarization (E-mode, generated by scalar-density perturbations) is of the order of 3 µK, while the current upper limits for the level of B-mode polarization are a fraction of μK, corresponding to a ratio between the amplitude of tensor perturbations and the amplitude of scalar perturbations (tensor-to-scalar ratio) $r < 0.044$ at 95% confidence level, combining data from the Planck satellite and the BICEP/Keck ground telescopes.[3–5] The B-mode of inflationary origin is observable at large angular scales, greater than 1.5°, and it exhibits local peaks in its power spectrum at degree angular scales (corresponding to multipoles of $\ell \simeq 80$) and on very large angular scales (corresponding to multipoles of $\ell \lesssim 10$)[1,6] due to processes taking place at recombination and reionization epochs, respectively.

LiteBIRD[7] aims at constraining the B-mode power spectrum of CMB polarization with sensitivity to both peaks in the large-scale angular power spectrum of the CMB polarization. In addition, thanks to its unprecedented target sensitivity, it will be able to reliably decouple the B-mode signal of primordial origin from the small angular-scale B-mode generated by gravitational lensing along the path of CMB photons to Earth.

LiteBIRD will observe the sky in 15 partially overlapped frequency bands from 34 to 448 GHz, with effective polarization sensitivity of 2 µK arcmin and an angular resolution of 31 arcmin at 140 GHz. The broad spectral coverage has been optimized to deal with the spectral complexity of the galactic polarized foregrounds. The observing strategy aims at continuously spinning the telescope boresight across the sky, while decoupling the tiny polarized sky-signals from instrumental contamination by means of polarization modulation. This is achieved through the use of spinning transmissive Half-Wave Plates (HWPs) located at the entrance of the optical system, providing 180° phase delay between the linear polarization components along the primary and secondary axes of the plates, ultimately rotating the polarization axis of the output radiation with respect to the input. This strategy provides polarized amplitude modulation at 4× the spinning frequency, with the non-negligible advantage of shifting the relevant electrical frequencies of the detectors signal away from the $1/f$ noise. Intrinsic limitations in the Half-Wave Plate achromaticity requirements, and an extended tradeoff analysis performed in the early stages of the development of LiteBIRD, have brought to the separation of the instrument into two mechanically, cryogenically and optically independent units, named the Low Frequency Telescope (LFT)[8] and

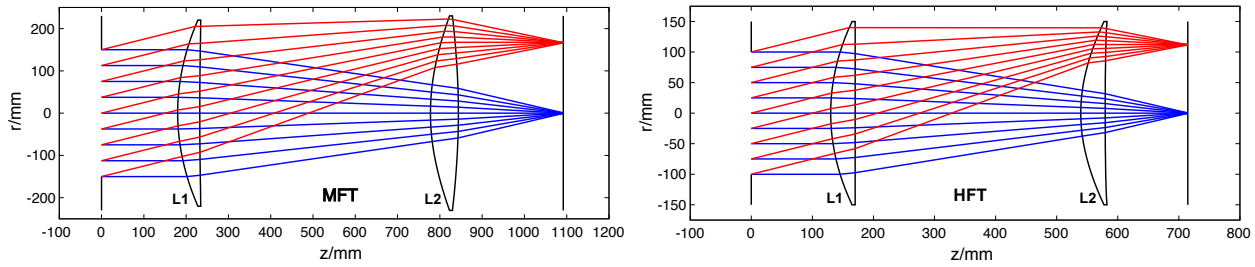

Figure 1. Ray diagrams of MFT (left) and HFT (right). The on-axis and off-axis fields (14 deg) are the blue and red rays, respectively. The telescope aperture is located at $z = 0$.

the Medium and High Frequency Telescope (MHFT).[9] In terms of optical configuration, the LFT features a reflective off-axis crossed-Dragone design, while the MHFT has been split into two optical tubes, each featuring a refractive, dual-lens axial configuration. The three optical systems feed focal plane assemblies populated with polarization-sensitive Transition Edge Sensors, for a total of 1210 multichroic pixels and 4508 independent detectors.

In the following sections, we summarize the baseline optical configurations and highlight the modeling steps towards a full numerical simulation of the MHFT telescopes.

2. SUMMARY OF BASELINE OPTICAL CONFIGURATIONS

The baseline optical configurations for the LiteBIRD MFT and HFT are summarized in table 1, and ray diagrams are shown in fig. 1. The two telescopes share the same refractive design philosophy, where the aperture stop is located at the entrance of the system, the image is formed from an objective lens (L1) and magnification, focal plane size, aberrations and telecentricity are adjusted through a field lens (L2). Polarization modulation is performed through a Polarization Modulation Unit (PMU), located in close vicinity of the aperture stop, providing uniform rotation of the HWP. In MHFT, the HWP technology is based on stacks of metal-mesh litographed grids[10,11] and the spinning is achieved through a superconducting magnetic bearing for optimum stability and control of the rotation parameters.[12] Both technologies have been validated in smaller aperture prototypes and are currently object of an extensive ESA-funded TRL advancement program. In addition, the same concept of PMU design, but with a larger (480 mm) diameter HWP than MFT, will be tested under environmentally representative conditions during the polar night flight of the SWIPE balloon-borne receiver.[13,14] For a more detailed description of the baseline optical performance, we refer the reader to a past edition of these proceedings.[15]

	MFT	HFT
Bandwidth	$89 - 224$ GHz	$166 - 448$ GHz
Multichroic detectors central frequencies	100/140/195, 119/166 GHz	195/280, 235/337, 402 GHz
Total n. of detectors	2074 $(1098 + 976)$	1354 $(508 + 508 + 338)$
Detector coupling	sinuous antenna + Si lenslet	horn+OMT
Stop diameter	300 mm	200 mm
Field of view	28°	28°
Focal ratio	2.2	2.2
Min-Max Strehl ratio at 14°	0.95 - 0.99	0.91 - 0.98

Table 1. Summary of baseline configurations for the 2-lens assemblies of MFT and HFT. Strehl ratios are computed at the edge of the nominal field of view and the min-max range refers to the shift in value across the telescope band.

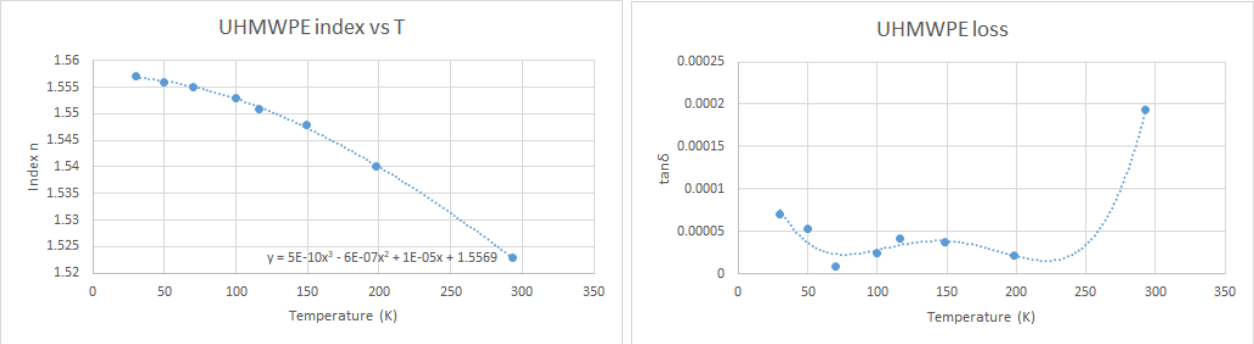

Figure 2. Measured refractive index and loss tangent of UHMW-PE as a function of temperature.

Initial designs for the MFT and HFT telescopes were implemented assuming n=1.52 for the UHMW-PE lens material at room temperature. Since the two MHFT telescopes will be cooled to 4.8 K, the final optical design will be based on the actual measurement of such properties at or close to this temperature. Recent work[16] has characterized the index and loss tangent for a typical sample of annealed UHMW-PE as a function of temperature, with the results shown in fig. 2. When the material is procured for the flight lenses, the flight design for the MHFT telescopes will be refined according to the actual index measured for this batch of material at cryogenic temperatures.

3. UPDATED PHYSICAL OPTICS SIMULATIONS

The ambitious target sensitivity of LiteBIRD (2 μK arcmin) demands unprecedented levels of calibration accuracy and systematic control. Calibration and systematics studies have pointed out to possible criticalities in the required/achievable level of knowledge of the beams away from the main lobe (near and far sidelobes).

Therefore, a quantitative test of the systematic effects due to miscalibration of the beams as a function of the angle from the boresight, of the focal plane location (and consequent beam asymmetry), of the polarization and of the optical frequency has been identified as a necessary step to push further the analysis of the calibration requirements. In addition, systematic studies are underway to evaluate the effectiveness of the scanning strategy in providing effective beam averaging through redundant scanning of the same sky region with different scan orientations (actually suppressing the level of asymmetry in the convolved maps at the price of a lower angular resolution), and to include the cross-polar response profiles in the time-domain simulation of the sky signals. The latter are particularly relevant in the far sidelobe region, where copolar and cross-polar beam responses are often comparable in amplitude and could possibly contribute to the ultimate determination of the beam calibration requirements in polarization. Such case studies are informative if the beam responses, assumed as their input, are accurate enough to capture the actual features of the MHFT telescopes. This has motivated the effort to include and validate multiple additional physical effects in the optical simulations, which will be described in the next section. Efforts towards the experimental validation of the optical modeling techniques through the characterization of reference designs (bread-board models, BBMs) are described in a separate paper.[17]

The first physical optics (PO) simulations have been presented in a past edition of these proceedings.[15] We summarize here the configuration of the simulation setup, in order to highlight the incremental improvements that have been included in the most recent iteration of the PO analysis. All the PO simulations have been performed with the GRASP software provided by Ticra*.

- nominal lenses have been included with no anti-reflection treatment on both surfaces, reproducing the baseline design and choice of refractive index used for ray-tracing.
- The optics tube has been treated as perfectly absorbing.

*https://www.ticra.com/software/grasp/

- A basic forebaffle geometry has been included by the definition of the input and output circular apertures; forebaffle walls have been treated as perfectly absorbing.
- simulations of the reverse path from the focal plane to the far field have been performed for the on-axis pixel and a limited selection of off-axis locations across the focal plane.
- feeds on representative focal plane locations have been assumed to be fully gaussian in shape.
- PO simulations have been run at 100 GHz and no band-averaging of single-frequency effects has been performed.

The co-polar beams output from this run have been implemented in the first version of the LiteBIRD Instrument Model (IMo) to run studies of the observing strategy, and have informed preliminary code optimizations in view of more refined mission planning and instrument modeling.

The original simulation design described above has been updated in the following aspects.

Feeds. Beam patterns for realistic coupling elements on the focal planes of the two telescopes have been generated with 3D Finite Element Modeling (FEM) analysis of the MFT and HFT coupling devices. MFT features planar sinuous antenna-coupled detectors, complemented by anti-reflection coated hemispherical silicon lenslets for an increased directivity; detector coupling for HFT has been proposed in the form of corrugated or spline-profiled circular horns feeding planar Ortho-Mode Transducers (OMTs). Both families of horn designs have been simulated at the HFT center frequencies with the same FEM technique as the MFT feeds. The output of the FEM simulation (performed with Ansys HFSS[†]) has been reprocessed in the format of azimuthal beam cuts and imported into the GRASP telescope model, to be used as a feed for the reverse-path propagation and the reconstruction of the beam pattern in the far-field. The phase center location for each beam pattern has been adjusted according to the nominal shift of its location with respect to the physical location of the detector array.

Forebaffle. As a followup to the already reported,[15] preliminary studies of the forebaffle aperture, a conical forebaffle with an entrance aperture of 421 mm and a length of 243 mm has been included in the MFT design. Forebaffle walls are treated as perfectly absorbing and the flare angle is still to be optimized (currently fixed at 14 °). The (conical) forebaffle wall is assumed to extend from the entrance aperture of the system all the way down to the aperture stop, close to the HWP location. In the presence of the PMU mechanism, such a design implies a protrusion of the forebaffle structure across the volume allocated for the PMU (see fig. 3). While conceptually feasible, such design is still pending approval from thermo-mechanical studies. Both the forebaffle apertures are modeled in GRASP as scatterers with the Physical Optics + Physical Theory of Diffraction (PO+PTD) solver for the calculation of currents and field propagation.

V-grooves As a first step towards the inclusion of potentially relevant effects in the far-sidelobe region of the beams, a large structure surrounding the MHFT has been included as an approximation of the first (and closest to the telescopes) layer of the V-groove assembly, designed to passively contribute to the cooldown of the scientific instrumentation below 30 K.[18] This structure is made of an octagon-shaped assembly of flat, fully reflective panels, coaxial to the payload spin axis[19] (see fig. 4, left panel).

By design, both the LFT and the MHFT have their boresight oriented at 50° from this axis,[7] so that the contribution of the V-grooves to the beam shapes is expected to be intrinsically asymmetric, depending on the azimuthal cut of the beams and on the focal plane location. While this section of the model is still highly prelimary, both in terms of design and of reliability assessment of its simulation in GRASP, its inclusion is helping to quantify the level of large scale beam asymmetry and features in the far sidelobe region.

The updated design used for the GRASP PO simulations is shown in the right panel of fig. 4 for the MFT. An equivalent design for the HFT, without the V-groove panels, is currently being tested against simulation

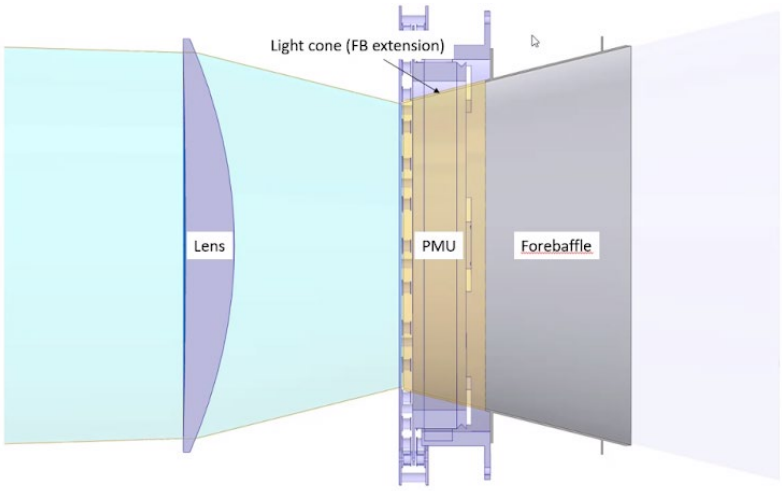

Figure 3. Forebaffle model and profile extension through the PMU (MFT design shown).

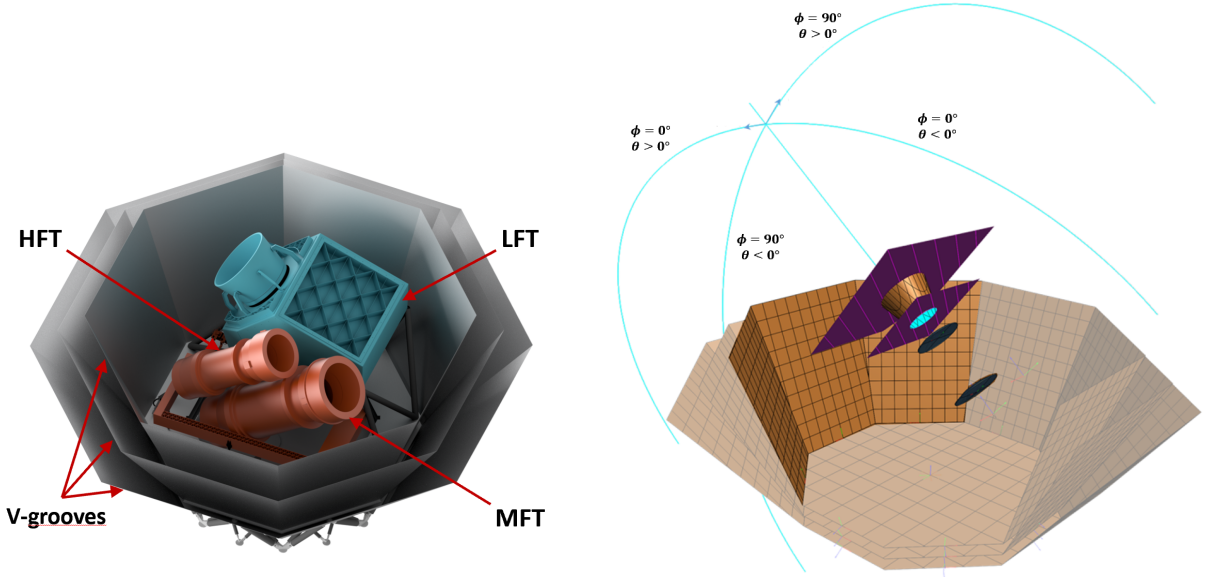

Figure 4. *Left:* 3d view of the LFT and MHFT assembly on the LiteBIRD payload module. *Right:* GRASP design of the MFT optical system and of the first V-groove layer. References for beam cuts with respect to the boresight are highlighted.

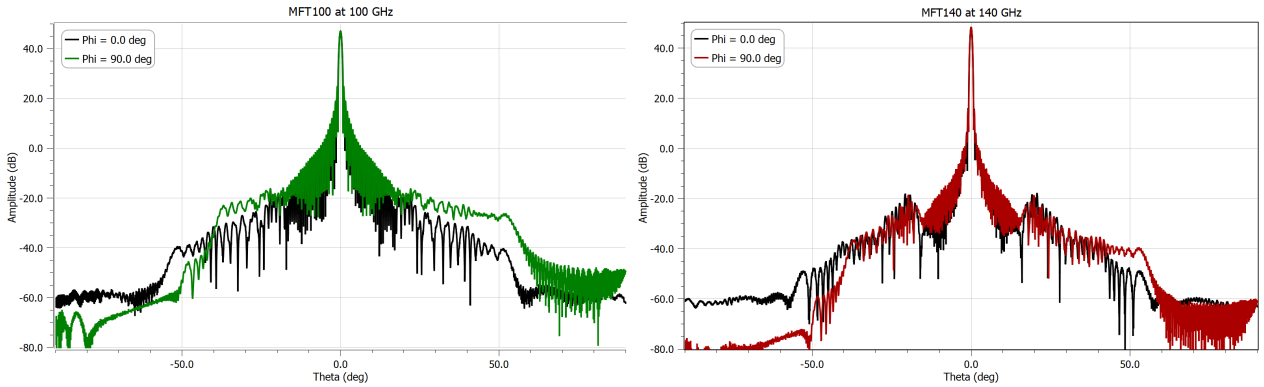

Figure 5. Newly simulated MFT beams for the 100 GHz and 140 GHz band-centers of MFT. See right panel of fig. 4 for the definition and orientation of the reference angles. The vertical beam cuts, corresponding to $\phi = 90°$, are clearly affected by additional power suppression and diffraction effects by the presence of the V-groove panels.

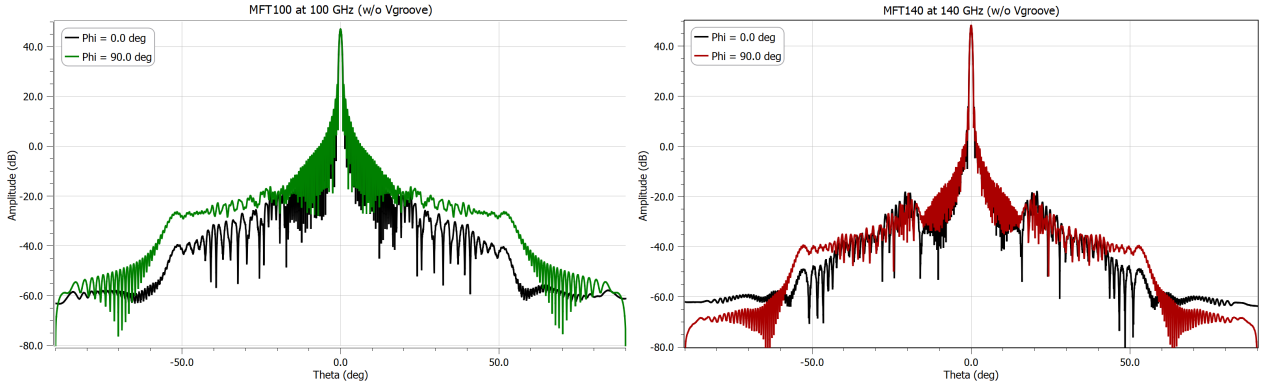

Figure 6. Same as fig. 5, but with the V-groove panels removed from the simulation.

parameters to check the robustness of the numerical results at high frequencies. A sample of the 2π-beam cuts generated for the MFT is shown in fig. 5 for the center frequencies of the 100 GHz and 140 GHz band-centers of MFT. Beam profiles are shown for the center of the MFT focal plane and for the two azimuthal cuts highlighted in the right panel of fig. 4. As a reference, the same MFT beam simulation is shown in the absence of the V-groove structure in fig. 6. A noticeable contribution from the panels is visible in the azimuthal cuts along the vertical plane, in the form of a stronger power suppression in the sidelobe region in the negative θ domain. At the moment of writing, only the three V-groove panels closest to the telescope boresight (and thus seen under the smallest angles from the telescope) are included in the simulation. In principle, no technical difficulties arise from the inclusion of the remaining V-groove structure, apart from a longer computing time. The current average running time for each of these simulations is approximately 45 min per focal plane location. A full update of the V-groove structure will therefore be included after checking and possibly validating the numerical robustness of the current generation of the MFT beams. The corresponding beam simulations for the HFT, on the other hand, are computationally more intensive: test runs for the lowest and highest HFT frequencies have required few tens of hours per focal plane location on the same hardware which we use for the MFT runs. For this reason, full HFT beam simulations in the presence of surrounding structure will be run only after consolidating the V-groove design and simulation setup with the MFT design. This stepped process will also be useful to confirm the compliance of the optical simulations with the format, precision and pointing information requirements set by the team taking care of the end-to-end simulation of observations.

[†]https://www.ansys.com/it-it/products/electronics/ansys-hfss

4. FUTURE WORK

A new run of end-to-end performance simulations of LiteBIRD is planned for the end of Summer 2022, and is meant to inform the MHFT Phase A2 report to CNES, which is coordinating the European effort for the MHFT development. The newly simulated beams are meant to be used as an input for this study. Further work in underway to advance in the level of complexity of the optical simulations. In particular:

- The current PO setup in GRASP is being optimized and run for the center frequencies of the 10 MFT+HFT bands. Feed simulations at ∼1 GHz spectral resolution are being prepared in order to iterate PO calculations across the bands. This step is needed to allow band-averaging and a more realistic assessment of frequency-sensitive beam features, which are likely to be integrated into smoother shapes in the sidelobes regions.
- Work is in progress with the LiteBIRD simulation team to identify reference locations on the focal planes of MFT and HFT to generate representative beam maps and assess beam-related systematics as a function of the focal-plane location and of the number of pixels located at each off-axis distance, while optimizing the amount of computational resources needed for optical simulations.
- Absorber plates, in the form of shaped surfaces coated with lossy dielectric material have been simulated and designed. Their laboratory characterization is in progress and the measured performance will be fed into dedicated Grasp simulations to account for imperfect absorption by the optics tube and by the surface around the cold aperture stop. Focus on the Eccosorb CR110 by Laird Technologies[‡] is presently dictated by the need for an off-the-shelf, robustly validated baseline material which has been designated as a reference for prototyping activities.
- Different candidate profiles for the forebaffle shape and structure are being designed and prepared for implementation in the optical simulations, along with the already mentioned specifications for the absorptive properties of their internally coated surfaces. For this effort, as well as for the studies related to realistic absorption properties of the optical tubes and the aperture stops, we are exploring a full-wave modeling approach based on the Method of Moments (MoM), available in GRASP as an alternative to PO+PTD.

ACKNOWLEDGMENTS

LiteBIRD (phase A) activities are supported by the following funding agencies: ISAS/JAXA, MEXT, JSPS, KEK (Japan); CSA (Canada); CNES, CNRS, CEA (France); DFG (Germany); ASI, INFN, INAF (Italy); RCN (Norway); AEI (Spain); SNSA, SRC (Sweden); NASA, DOE (USA).

REFERENCES

[1] Seljak, U. and Zaldarriaga, M., "Signature of gravity waves in the polarization of the microwave background," *Phys. Rev. Lett.* **78**, 2054–2057 (Mar 1997).

[2] Kamionkowski, M. and Kovetz, E. D., "The Quest for B Modes from Inflationary Gravitational Waves," *Annu. Rev. Astron. Astr.* **54**(1), 227–269 (2016).

[3] Planck Collaboration, Aghanim, N., Akrami, Y., Arroja, F., Ashdown, M., Aumont, J., Baccigalupi, C., Ballardini, M., Banday, A. J., Barreiro, R. B., Bartolo, N., Basak, S., Battye, R., Benabed, K., Bernard, J. P., Bersanelli, M., Bielewicz, P., Bock, J. J., Bond, J. R., Borrill, J., Bouchet, F. R., Boulanger, F., Bucher, M., Burigana, C., Butler, R. C., Calabrese, E., Cardoso, J. F., Carron, J., Casaponsa, B., Challinor, A., Chiang, H. C., Colombo, L. P. L., Combet, C., Contreras, D., Crill, B. P., Cuttaia, F., de Bernardis, P., de Zotti, G., Delabrouille, J., Delouis, J. M., Désert, F. X., Di Valentino, E., Dickinson, C., Diego, J. M., Donzelli, S., Doré, O., Douspis, M., Ducout, A., Dupac, X., Efstathiou, G., Elsner, F., Enßlin, T. A., Eriksen, H. K., Falgarone, E., Fantaye, Y., Fergusson, J., Fernandez-Cobos, R., Finelli, F., Forastieri, F., Frailis, M., Franceschi, E., Frolov, A., Galeotta, S., Galli, S., Ganga, K., Génova-Santos, R. T., Gerbino, M., Ghosh, T., González-Nuevo, J., Górski, K. M., Gratton, S., Gruppuso, A., Gudmundsson, J. E., Hamann, J., Handley, W., Hansen, F. K., Helou, G., Herranz, D., Hildebrandt, S. R., Hivon, E., Huang, Z., Jaffe,

[‡]https://www.laird.com/

A. H., Jones, W. C., Karakci, A., Keihänen, E., Keskitalo, R., Kiiveri, K., Kim, J., Kisner, T. S., Knox, L., Krachmalnicoff, N., Kunz, M., Kurki-Suonio, H., Lagache, G., Lamarre, J. M., Langer, M., Lasenby, A., Lattanzi, M., Lawrence, C. R., Le Jeune, M., Leahy, J. P., Lesgourgues, J., Levrier, F., Lewis, A., Liguori, M., Lilje, P. B., Lilley, M., Lindholm, V., López-Caniego, M., Lubin, P. M., Ma, Y. Z., Macías-Pérez, J. F., Maggio, G., Maino, D., Mandolesi, N., Mangilli, A., Marcos-Caballero, A., Maris, M., Martin, P. G., Martinelli, M., Martínez-González, E., Matarrese, S., Mauri, N., McEwen, J. D., Meerburg, P. D., Meinhold, P. R., Melchiorri, A., Mennella, A., Migliaccio, M., Millea, M., Mitra, S., Miville-Deschênes, M. A., Molinari, D., Moneti, A., Montier, L., Morgante, G., Moss, A., Mottet, S., Münchmeyer, M., Natoli, P., Nørgaard-Nielsen, H. U., Oxborrow, C. A., Pagano, L., Paoletti, D., Partridge, B., Patanchon, G., Pearson, T. J., Peel, M., Peiris, H. V., Perrotta, F., Pettorino, V., Piacentini, F., Polastri, L., Polenta, G., Puget, J. L., Rachen, J. P., Reinecke, M., Remazeilles, M., Renault, C., Renzi, A., Rocha, G., Rosset, C., Roudier, G., Rubiño-Martín, J. A., Ruiz-Granados, B., Salvati, L., Sandri, M., Savelainen, M., Scott, D., Shellard, E. P. S., Shiraishi, M., Sirignano, C., Sirri, G., Spencer, L. D., Sunyaev, R., Suur-Uski, A. S., Tauber, J. A., Tavagnacco, D., Tenti, M., Terenzi, L., Toffolatti, L., Tomasi, M., Trombetti, T., Valiviita, J., Van Tent, B., Vibert, L., Vielva, P., Villa, F., Vittorio, N., Wandelt, B. D., Wehus, I. K., White, M., White, S. D. M., Zacchei, A., and Zonca, A., "Planck 2018 results. I. Overview and the cosmological legacy of Planck," *Astronomy and Astrophysics* **641**, A1 (Sept. 2020).

[4] Tristram, M., Banday, A. J., Górski, K. M., Keskitalo, R., Lawrence, C. R., Andersen, K. J., Barreiro, R. B., Borrill, J., Eriksen, H. K., Fernandez-Cobos, R., Kisner, T. S., Martínez-González, E., Partridge, B., Scott, D., Svalheim, T. L., Thommesen, H., and Wehus, I. K., "Planck constraints on the tensor-to-scalar ratio," *Astronomy and Astrophysics* **647**, A128 (Mar. 2021).

[5] Ade, P. A. R., Ahmed, Z., Aikin, R. W., Alexander, K. D., Barkats, D., Benton, S. J., Bischoff, C. A., Bock, J. J., Bowens-Rubin, R., Brevik, J. A., Buder, I., Bullock, E., Buza, V., Connors, J., Cornelison, J., Crill, B. P., Crumrine, M., Dierickx, M., Duband, L., Dvorkin, C., Filippini, J. P., Fliescher, S., Grayson, J., Hall, G., Halpern, M., Harrison, S., Hildebrandt, S. R., Hilton, G. C., Hui, H., Irwin, K. D., Kang, J., Karkare, K. S., Karpel, E., Kaufman, J. P., Keating, B. G., Kefeli, S., Kernasovskiy, S. A., Kovac, J. M., Kuo, C. L., Larsen, N. A., Lau, K., Leitch, E. M., Lueker, M., Megerian, K. G., Moncelsi, L., Namikawa, T., Netterfield, C. B., Nguyen, H. T., O'Brient, R., Ogburn, R. W., Palladino, S., Pryke, C., Racine, B., Richter, S., Schillaci, A., Schwarz, R., Sheehy, C. D., Soliman, A., St. Germaine, T., Staniszewski, Z. K., Steinbach, B., Sudiwala, R. V., Teply, G. P., Thompson, K. L., Tolan, J. E., Tucker, C., Turner, A. D., Umiltà, C., Vieregg, A. G., Wandui, A., Weber, A. C., Wiebe, D. V., Willmert, J., Wong, C. L., Wu, W. L. K., Yang, H., Yoon, K. W., Zhang, C., Keck Array, and bicep2 Collaborations, "Constraints on Primordial Gravitational Waves Using Planck, WMAP, and New BICEP2/Keck Observations through the 2015 Season," *Phys. Rev. Lett.* **121**, 221301 (Nov. 2018).

[6] Zaldarriaga, M. and Seljak, U. c. v., "All-sky analysis of polarization in the microwave background," *Phys. Rev. D* **55**, 1830–1840 (Feb 1997).

[7] LiteBIRD Collaboration, Allys, E., Arnold, K., Aumont, J., Aurlien, R., Azzoni, S., Baccigalupi, C., Banday, A. J., Banerji, R., Barreiro, R. B., Bartolo, N., Bautista, L., Beck, D., Beckman, S., Bersanelli, M., Boulanger, F., Brilenkov, M., Bucher, M., Calabrese, E., Campeti, P., Carones, A., Casas, F. J., Catalano, A., Chan, V., Cheung, K., Chinone, Y., Clark, S. E., Columbro, F., D'Alessandro, G., de Bernardis, P., de Haan, T., de la Hoz, E., De Petris, M., Della Torre, S., Diego-Palazuelos, P., Dotani, T., Duval, J. M., Elleflot, T., Eriksen, H. K., Errard, J., Essinger-Hileman, T., Finelli, F., Flauger, R., Franceschet, C., Fuskeland, U., Galloway, M., Ganga, K., Gerbino, M., Gervasi, M., Génova-Santos, R. T., Ghigna, T., Giardiello, S., Gjerløw, E., Grain, J., Grupp, F., Gruppuso, A., Gudmundsson, J. E., Halverson, N. W., Hargrave, P., Hasebe, T., Hasegawa, M., Hazumi, M., Henrot-Versillé, S., Hensley, B., Hergt, L. T., Herman, D., Hivon, E., Hlozek, R. A., Hornsby, A. L., Hoshino, Y., Hubmayr, J., Ichiki, K., Iida, T., Imada, H., Ishino, H., Jaehnig, G., Katayama, N., Kato, A., Keskitalo, R., Kisner, T., Kobayashi, Y., Kogut, A., Kohri, K., Komatsu, E., Komatsu, K., Konishi, K., Krachmalnicoff, N., Kuo, C. L., Lamagna, L., Lattanzi, M., Lee, A. T., Leloup, C., Levrier, F., Linder, E., Luzzi, G., Macias-Perez, J., Maffei, B., Maino, D., Mandelli, S., Martínez-González, E., Masi, S., Massa, M., Matarrese, S., Matsuda, F. T., Matsumura, T., Mele, L., Migliaccio, M., Minami, Y., Moggi, A., Montgomery, J., Montier, L., Morgante, G., Mot, B., Nagano, Y., Nagasaki, T., Nagata, R., Nakano, R., Namikawa, T., Nati, F., Natoli, P., Nerval, S., Noviello, F., Odagiri,

K., Oguri, S., Ohsaki, H., Pagano, L., Paiella, A., Paoletti, D., Passerini, A., Patanchon, G., Piacentini, F., Piat, M., Polenta, G., Poletti, D., Prouvé, T., Puglisi, G., Rambaud, D., Raum, C., Realini, S., Reinecke, M., Remazeilles, M., Ritacco, A., Roudil, G., Rubino-Martin, J. A., Russell, M., Sakurai, H., Sakurai, Y., Sasaki, M., Scott, D., Sekimoto, Y., Shinozaki, K., Shiraishi, M., Shirron, P., Signorelli, G., Spinella, F., Stever, S., Stompor, R., Sugiyama, S., Sullivan, R. M., Suzuki, A., Svalheim, T. L., Switzer, E., Takaku, R., Takakura, H., Takase, Y., Tartari, A., Terao, Y., Thermeau, J., Thommesen, H., Thompson, K. L., Tomasi, M., Tominaga, M., Tristram, M., Tsuji, M., Tsujimoto, M., Vacher, L., Vielva, P., Vittorio, N., Wang, W., Watanuki, K., Wehus, I. K., Weller, J., Westbrook, B., Wilms, J., Wollack, E. J., Yumoto, J., and Zannoni, M., "Probing cosmic inflation with the litebird cosmic microwave background polarization survey," (2022).

[8] Sekimoto, Y., Ade, P. A. R., Adler, A., Allys, E., Arnold, K., Auguste, D., Aumont, J., Aurlien, R., Austermann, J., Baccigalupi, C., Banday, A. J., Banerji, R., Barreiro, R. B., Basak, S., Beall, J., Beck, D., Beckman, S., Bermejo, J., de Bernardis, P., Bersanelli, M., Bonis, J., Borrill, J., Boulanger, F., Bounissou, S., Brilenkov, M., Brown, M., Bucher, M., Calabrese, E., Campeti, P., Carones, A., Casas, F. J., Challinor, A., Chan, V., Cheung, K., Chinone, Y., Cliche, J. F., Colombo, L., Columbro, F., Cubas, J., Cukierman, A., Curtis, D., D'Alessandro, G., Dachlythra, N., Petris, M. D., Dickinson, C., Diego-Palazuelos, P., Dobbs, M., Dotani, T., Duband, L., Duff, S., Duval, J. M., Ebisawa, K., Elleflot, T., Eriksen, H. K., Errard, J., Essinger-Hileman, T., Finelli, F., Flauger, R., Franceschet, C., Fuskeland, U., Galloway, M., Ganga, K., Gao, J. R., Genova-Santos, R., Gerbino, M., Gervasi, M., Ghigna, T., Gjerløw, E., Gradziel, M. L., Grain, J., Grupp, F., Gruppuso, A., Gudmundsson, J. E., de Haan, T., Halverson, N. W., Hargrave, P., Hasebe, T., Hasegawa, M., Hattori, M., Hazumi, M., Henrot-Versillé, S., Herman, D., Herranz, D., Hill, C. A., Hilton, G., Hirota, Y., Hivon, E., Hlozek, R. A., Hoshino, Y., de la Hoz, E., Hubmayr, J., Ichiki, K., iida, T., Imada, H., Ishimura, K., Ishino, H., Jaehnig, G., Kaga, T., Kashima, S., Katayama, N., Kato, A., Kawasaki, T., Keskitalo, R., Kisner, T., Kobayashi, Y., Kogiso, N., Kogut, A., Kohri, K., Komatsu, E., Komatsu, K., Konishi, K., Krachmalnicoff, N., Kreykenbohm, I., Kuo, C. L., Kushino, A., Lamagna, L., Lanen, J. V., Lattanzi, M., Lee, A. T., Leloup, C., Levrier, F., Linder, E., Louis, T., Luzzi, G., Maciaszek, T., Maffei, B., Maino, D., Maki, M., Mandelli, S., Martinez-Gonzalez, E., Masi, S., Matsumura, T., Mennella, A., Migliaccio, M., Minanmi, Y., Mitsuda, K., Montgomery, J., Montier, L., Morgante, G., Mot, B., Murata, Y., Murphy, J. A., Nagai, M., Nagano, Y., Nagasaki, T., Nagata, R., Nakamura, S., Namikawa, T., Natoli, P., Nerval, S., Nishibori, T., Nishino, H., O'Sullivan, C., Ogawa, H., Ogawa, H., Oguri, S., Ohsaki, H., Ohta, I. S., Okada, N., Okada, N., Pagano, L., Paiella, A., Paoletti, D., Patanchon, G., Peloton, J., Piacentini, F., Pisano, G., Polenta, G., Poletti, D., Prouvé, T., Puglisi, G., Rambaud, D., Raum, C., Realini, S., Reinecke, M., Remazeilles, M., Ritacco, A., Roudil, G., Rubino-Martin, J. A., Russell, M., Sakurai, H., Sakurai, Y., Sandri, M., Sasaki, M., Savini, G., Scott, D., Seibert, J., Sherwin, B., Shinozaki, K., Shiraishi, M., Shirron, P., Signorelli, G., Smecher, G., Stever, S., Stompor, R., Sugai, H., Sugiyama, S., Suzuki, A., Suzuki, J., Svalheim, T. L., Switzer, E., Takaku, R., Takakura, H., Takakura, S., Takase, Y., Takeda, Y., Tartari, A., Taylor, E., Terao, Y., Thommesen, H., Thompson, K. L., Thorne, B., Toda, T., Tomasi, M., Tominaga, M., Trappe, N., Tristram, M., Tsuji, M., Tsujimoto, M., Tucker, C., Ullom, J., Vermeulen, G., Vielva, P., Villa, F., Vissers, M., Vittorio, N., Wehus, I., Weller, J., Westbrook, B., Wilms, J., Winter, B., Wollack, E. J., Yamasaki, N. Y., Yoshida, T., Yumoto, J., Zannoni, M., and Zonca, A., "Concept design of low frequency telescope for CMB B-mode polarization satellite LiteBIRD," in [*Millimeter, Submillimeter, and Far-Infrared Detectors and Instrumentation for Astronomy X*], Zmuidzinas, J. and Gao, J.-R., eds., **11453**, 189 – 209, International Society for Optics and Photonics, SPIE (2020).

[9] Montier, L., Mot, B., de Bernardis, P., Maffei, B., Pisano, G., Columbro, F., Gudmundsson, J. E., Henrot-Versillé, S., Lamagna, L., Montgomery, J., Prouvé, T., Russell, M., Savini, G., Stever, S., Thompson, K. L., Tsujimoto, M., Tucker, C., Westbrook, B., Ade, P. A. R., Adler, A., Allys, E., Arnold, K., Auguste, D., Aumont, J., Aurlien, R., Austermann, J., Baccigalupi, C., Banday, A. J., Banerji, R., Barreiro, R. B., Basak, S., Beall, J., Beck, D., Beckman, S., Bermejo, J., Bersanelli, M., Bonis, J., Borrill, J., Boulanger, F., Bounissou, S., Brilenkov, M., Brown, M., Bucher, M., Calabrese, E., Campeti, P., Carones, A., Casas, F. J., Challinor, A., Chan, V., Cheung, K., Chinone, Y., Cliche, J. F., Colombo, L., Cubas, J., Cukierman, A., Curtis, D., D'Alessandro, G., Dachlythra, N., Petris, M. D., Dickinson, C., Diego-Palazuelos, P., Dobbs, M., Dotani, T., Duband, L., Duff, S., Duval, J. M., Ebisawa, K., Elleflot, T., Eriksen, H. K., Errard, J., Essinger-Hileman, T., Finelli, F., Flauger, R., Franceschet, C., Fuskeland, U., Galloway, M., Ganga, K.,

Gao, J. R., Genova-Santos, R., Gerbino, M., Gervasi, M., Ghigna, T., Gjerløw, E., Gradziel, M. L., Grain, J., Grupp, F., Gruppuso, A., de Haan, T., Halverson, N. W., Hargrave, P., Hasebe, T., Hasegawa, M., Hattori, M., Hazumi, M., Herman, D., Herranz, D., Hill, C. A., Hilton, G., Hirota, Y., Hivon, E., Hlozek, R. A., Hoshino, Y., de la Hoz, E., Hubmayr, J., Ichiki, K., Iida, T., Imada, H., Ishimura, K., Ishino, H., Jaehnig, G., Kaga, T., Kashima, S., Katayama, N., Kato, A., Kawasaki, T., Keskitalo, R., Kisner, T., Kobayashi, Y., Kogiso, N., Kogut, A., Kohri, K., Komatsu, E., Komatsu, K., Konishi, K., Krachmalnicoff, N., Kreykenbohm, I., Kuo, C. L., Kushino, A., Lanen, J. V., Lattanzi, M., Lee, A. T., Leloup, C., Levrier, F., Linder, E., Louis, T., Luzzi, G., Maciaszek, T., Maino, D., Maki, M., Mandelli, S., Martinez-Gonzalez, E., Masi, S., Matsumura, T., Mennella, A., Migliaccio, M., Minami, Y., Mitsuda, K., Morgante, G., Murata, Y., Murphy, J. A., Nagai, M., Nagano, Y., Nagasaki, T., Nagata, R., Nakamura, S., Namikawa, T., Natoli, P., Nerval, S., Nishibori, T., Nishino, H., O'Sullivan, C., Ogawa, H., Ogawa, H., Oguri, S., Ohsaki, H., Ohta, I. S., Okada, N., Okada, N., Pagano, L., Paiella, A., Paoletti, D., Patanchon, G., Peloton, J., Piacentini, F., Polenta, G., Poletti, D., Puglisi, G., Rambaud, D., Raum, C., Realini, S., Reinecke, M., Remazeilles, M., Ritacco, A., Roudil, G., Rubino-Martin, J. A., Sakurai, H., Sakurai, Y., Sandri, M., Sasaki, M., Scott, D., Seibert, J., Sekimoto, Y., Sherwin, B., Shinozaki, K., Shiraishi, M., Shirron, P., Signorelli, G., Smecher, G., Stompor, R., Sugai, H., Sugiyama, S., Suzuki, A., Suzuki, J., Svalheim, T. L., Switzer, E., Takaku, R., Takakura, H., Takakura, S., Takase, Y., Takeda, Y., Tartari, A., Taylor, E., Terao, Y., Thommesen, H., Thorne, B., Toda, T., Tomasi, M., Tominaga, M., Trappe, N., Tristram, M., Tsuji, M., Ullom, J., Vermeulen, G., Vielva, P., Villa, F., Vissers, M., Vittorio, N., Wehus, I., Weller, J., Wilms, J., Winter, B., Wollack, E. J., Yamasaki, N. Y., Yoshida, T., Yumoto, J., Zannoni, M., and Zonca, A., "Overview of the medium and high frequency telescopes of the LiteBIRD space mission," in [*Space Telescopes and Instrumentation 2020: Optical, Infrared, and Millimeter Wave*], Lystrup, M., Perrin, M. D., Batalha, N., Siegler, N., and Tong, E. C., eds., **11443**, 451 – 471, International Society for Optics and Photonics, SPIE (2020).

[10] Pisano, G., Maffei, B., Ade, P. A. R., de Bernardis, P., de Maagt, P., Ellison, B., Henry, M., Ng, M. W., Schortt, B., and Tucker, C., "Multi-octave metamaterial reflective half-wave plate for millimeter and sub-millimeter wave applications," *Applied Optics* **55**, 10255 (Dec. 2016).

[11] Pisano, G., Ritacco, A., Monfardini, A., Tucker, C., Ade, P. A. R., Shitvov, A., Benoit, A., Calvo, M., Catalano, A., Goupy, J., Leclercq, S., Macias-Perez, J., Andrianasolo, A., and Ponthieu, N., "Development and application of metamaterial-based half-wave plates for the nika and nika2 polarimeters," *A&A* **658**, A24 (2022).

[12] Columbro, F., de Bernardis, P., Lamagna, L., Masi, S., Paiella, A., Piacentini, F., and Pisano, G., "A polarization modulator unit for the mid- and high-frequency telescopes of the LiteBIRD mission," in [*Space Telescopes and Instrumentation 2020: Optical, Infrared, and Millimeter Wave*], Lystrup, M., Perrin, M. D., Batalha, N., Siegler, N., and Tong, E. C., eds., **11443**, 1113 – 1128, International Society for Optics and Photonics, SPIE (2020).

[13] Columbro, F., Battistelli, E. S., Coppolecchia, A., D'Alessandro, G., de Bernardis, P., Lamagna, L., Masi, S., Pagano, L., Paiella, A., Piacentini, F., and Presta, G., "The short wavelength instrument for the polarization explorer balloon-borne experiment: Polarization modulation issues," *Astron. Nachr.* **340**, 83–88 (Jan. 2019).

[14] Addamo, G., Ade, P., Baccigalupi, C., Baldini, A., Battaglia, P., Battistelli, E., Baù, A., de Bernardis, P., Bersanelli, M., Biasotti, M., Boscaleri, A., Caccianiga, B., Caprioli, S., Cavaliere, F., Cei, F., Cleary, K., Columbro, F., Coppi, G., Coppolecchia, A., Cuttaia, F., D'Alessandro, G., Gasperis, G. D., Petris, M. D., Fafone, V., Farsian, F., Barusso, L. F., Fontanelli, F., Franceschet, C., Gaier, T., Galli, L., Gatti, F., Genova-Santos, R., Gerbino, M., Gervasi, M., Ghigna, T., Grosso, D., Gruppuso, A., Gualtieri, R., Incardona, F., Jones, M., Kangaslahti, P., Krachmalnicoff, N., Lamagna, L., Lattanzi, M., López-Caraballo, C., Lumia, M., Mainini, R., Maino, D., Mandelli, S., Maris, M., Masi, S., Matarrese, S., May, A., Mele, L., Mena, P., Mennella, A., Molina, R., Molinari, D., Morgante, G., Natale, U., Nati, F., Natoli, P., Pagano, L., Paiella, A., Panico, F., Paonessa, F., Paradiso, S., Passerini, A., de Taoro, M. P., Peverini, O., Pezzotta, F., Piacentini, F., Piccirillo, L., Pisano, G., Polenta, G., Poletti, D., Presta, G., Realini, S., Reyes, N., Rocchi, A., Rubino-Martin, J., Sandri, M., Sartor, S., Schillaci, A., Signorelli, G., Siri, B., Soria, M., Spinella, F., Tapia, V., Tartari, A., Taylor, A., Terenzi, L., Tomasi, M., Tommasi, E., Tucker, C., Vaccaro, D., Vigano, D., Villa, F., Virone, G., Vittorio, N., Volpe, A., Watkins, R., Zacchei, A., and Zannoni, M., "The large

scale polarization explorer (LSPE) for CMB measurements: performance forecast," *Journal of Cosmology and Astroparticle Physics* **2021**, 008 (aug 2021).

[15] Sekimoto, Y., Ade, P. A. R., Adler, A., Allys, E., Arnold, K., Auguste, D., Aumont, J., Aurlien, R., Austermann, J., Baccigalupi, C., Banday, A. J., Banerji, R., Barreiro, R. B., Basak, S., Beall, J., Beck, D., Beckman, S., Bermejo, J., de Bernardis, P., Bersanelli, M., Bonis, J., Borrill, J., Boulanger, F., Bounissou, S., Brilenkov, M., Brown, M., Bucher, M., Calabrese, E., Campeti, P., Carones, A., Casas, F. J., Challinor, A., Chan, V., Cheung, K., Chinone, Y., Cliche, J. F., Colombo, L., Columbro, F., Cubas, J., Cukierman, A., Curtis, D., D'Alessandro, G., Dachlythra, N., Petris, M. D., Dickinson, C., Diego-Palazuelos, P., Dobbs, M., Dotani, T., Duband, L., Duff, S., Duval, J. M., Ebisawa, K., Elleflot, T., Eriksen, H. K., Errard, J., Essinger-Hileman, T., Finelli, F., Flauger, R., Franceschet, C., Fuskeland, U., Galloway, M., Ganga, K., Gao, J. R., Genova-Santos, R., Gerbino, M., Gervasi, M., Ghigna, T., Gjerløw, E., Gradziel, M. L., Grain, J., Grupp, F., Gruppuso, A., Gudmundsson, J. E., de Haan, T., Halverson, N. W., Hargrave, P., Hasebe, T., Hasegawa, M., Hattori, M., Hazumi, M., Henrot-Versillé, S., Herman, D., Herranz, D., Hill, C. A., Hilton, G., Hirota, Y., Hivon, E., Hlozek, R. A., Hoshino, Y., de la Hoz, E., Hubmayr, J., Ichiki, K., iida, T., Imada, H., Ishimura, K., Ishino, H., Jaehnig, G., Kaga, T., Kashima, S., Katayama, N., Kato, A., Kawasaki, T., Keskitalo, R., Kisner, T., Kobayashi, Y., Kogiso, N., Kogut, A., Kohri, K., Komatsu, E., Komatsu, K., Konishi, K., Krachmalnicoff, N., Kreykenbohm, I., Kuo, C. L., Kushino, A., Lamagna, L., Lanen, J. V., Lattanzi, M., Lee, A. T., Leloup, C., Levrier, F., Linder, E., Louis, T., Luzzi, G., Maciaszek, T., Maffei, B., Maino, D., Maki, M., Mandelli, S., Martinez-Gonzalez, E., Masi, S., Matsumura, T., Mennella, A., Migliaccio, M., Minanmi, Y., Mitsuda, K., Montgomery, J., Montier, L., Morgante, G., Mot, B., Murata, Y., Murphy, J. A., Nagai, M., Nagano, Y., Nagasaki, T., Nagata, R., Nakamura, S., Namikawa, T., Natoli, P., Nerval, S., Nishibori, T., Nishino, H., O'Sullivan, C., Ogawa, H., Ogawa, H., Oguri, S., Ohsaki, H., Ohta, I. S., Okada, N., Okada, N., Pagano, L., Paiella, A., Paoletti, D., Patanchon, G., Peloton, J., Piacentini, F., Pisano, G., Polenta, G., Poletti, D., Prouvé, T., Puglisi, G., Rambaud, D., Raum, C., Realini, S., Reinecke, M., Remazeilles, M., Ritacco, A., Roudil, G., Rubino-Martin, J. A., Russell, M., Sakurai, H., Sakurai, Y., Sandri, M., Sasaki, M., Savini, G., Scott, D., Seibert, J., Sherwin, B., Shinozaki, K., Shiraishi, M., Shirron, P., Signorelli, G., Smecher, G., Stever, S., Stompor, R., Sugai, H., Sugiyama, S., Suzuki, A., Suzuki, J., Svalheim, T. L., Switzer, E., Takaku, R., Takakura, H., Takakura, S., Takase, Y., Takeda, Y., Tartari, A., Taylor, E., Terao, Y., Thommesen, H., Thompson, K. L., Thorne, B., Toda, T., Tomasi, M., Tominaga, M., Trappe, N., Tristram, M., Tsuji, M., Tsujimoto, M., Tucker, C., Ullom, J., Vermeulen, G., Vielva, P., Villa, F., Vissers, M., Vittorio, N., Wehus, I., Weller, J., Westbrook, B., Wilms, J., Winter, B., Wollack, E. J., Yamasaki, N. Y., Yoshida, T., Yumoto, J., Zannoni, M., and Zonca, A., "Concept design of low frequency telescope for CMB B-mode polarization satellite LiteBIRD," in [*Millimeter, Submillimeter, and Far-Infrared Detectors and Instrumentation for Astronomy X*], Zmuidzinas, J. and Gao, J.-R., eds., **11453**, 189 – 209, International Society for Optics and Photonics, SPIE (2020).

[16] Shitvov, A. et al., "Broadband coated lens solutions for FIR-mm-wave instruments," in [*Millimeter, Submillimeter, and Far-Infrared Detectors and Instrumentation for Astronomy XI*], **12190-19**, International Society for Optics and Photonics, SPIE (2022).

[17] Franceschet, C. et al., "The optical bread-board models of the LiteBIRD Medium & High Frequency Telescope," in [*Millimeter, Submillimeter, and Far-Infrared Detectors and Instrumentation for Astronomy XI*], **12190-127**, International Society for Optics and Photonics, SPIE (2022).

[18] Odagiri, K. et al., "Cryogenic thermal design and analysis for LiteBIRD payload module," in [*Space Telescopes and Instrumentation 2022: Optical, Infrared, and Millimeter Wave*], **12180-68**, International Society for Optics and Photonics, SPIE (2022).

[19] Oguri, S. et al., "Mechanical Design and structural analysis for LiteBIRD low frequency telescope," in [*Space Telescopes and Instrumentation 2022: Optical, Infrared, and Millimeter Wave*], **12180-230**, International Society for Optics and Photonics, SPIE (2022).